Journal of Plant Physiology 274 (2022) 153730

Contents lists available at ScienceDirect

Journal of Plant Physiology

journal homepage: www.elsevier.com/locate/jplph

Characterization and impact of sunflower plastidial octanoyltransferases (*Helianthus annuus* L.) on oil composition

Raquel Martins-Noguerol [a,b], Sebastien Acket [c], Manuel Adrián Troncoso-Ponce [c], Rafael Garcés [a], Mónica Venegas-Calerón [a], Joaquín J. Salas [a], Enrique Martínez-Force [a], Antonio Javier Moreno-Pérez [a,*]

[a] Instituto de la Grasa-CSIC, Building 46, UPO Campus, Ctra. de Utrera km 1, 41013, Seville, Spain
[b] Departamento de Biología Vegetal y Ecología, Facultad de Biología, Universidad de Sevilla, Seville, Spain
[c] Université de Technologie de Compiègne, Génie Enzymatique et Cellulaire (GEC), UMR-CNRS 7025, CS 60319, 60203, Compiègne Cedex, France

ARTICLE INFO

Keywords:
Sunflower
Octanoyltransferase
Protein lipoylation
Lipoic acid

ABSTRACT

Prosthetic lipoyl groups are essential for the metabolic activity of several multienzyme complexes in most organisms. In plants, octanoyltransferase (LIP2) and lipoyl synthase (LIP1) enzymes in the mitochondria and plastids participate in the *de novo* synthesis of lipoic acid, and in the attachment of the lipoyl cofactors to their specific targets. In plastids, the lipoylated pyruvate dehydrogenase complex catalyzes the synthesis of the acetyl-CoA that is required for *de novo* fatty acid synthesis. Since lipoic acid transport across plastid membranes has not been demonstrated, these organelles require specific plastidial LIP1 and LIP2 activities for the *in situ* synthesis of this cofactor. Previously, one essential LIP1 enzyme and two redundant LIP2 enzymes have been identified within Arabidopsis chloroplasts. In this study, two plastidial sunflower (*Helianthus annuus* L.) LIP2 genes (*HaLIP2p1* and *HaLIP2p2*) were identified, cloned and characterized. The expression of these genes in different tissues was studied and the tertiary structure of the peptides they encode was modeled by protein docking. These genes were overexpressed in *Escherichia coli* and their impact on bacterial fatty acid synthesis was studied. Finally, transgenic Arabidopsis plants overexpressing *HaLIP2p1* were generated and their seed lipid profiles analyzed. The lipid composition of the transgenic seeds, particularly their TAG species, differed from that of wild-type plants, revealing a relationship between lipoic acid synthesis and the accumulation of storage lipids in Arabidopsis seeds.

1. Introduction

Plastids are the major site of fatty acid synthesis in plants (Ohlrogge et al., 1979), a process in which acetyl-CoA represents the building block of this biosynthetic process (Schwender et al., 2004; Alonso et al., 2007). Acetyl-CoA is produced through the activity of the plastidial pyruvate dehydrogenase complex (PDH), which catalyzes the oxidative decarboxylation of pyruvate to acetyl-CoA. The E2 subunit (E2-PDH) of this complex is a dihydrolipoamide dehydrogenase that must be lipoylated to function correctly. The lipoic acid (LA: thioctic acid or 6,8-dithiooctanoic acid) required for this activation is a modified form of octanoic acid that contains two thiol substituents at the Δ6 and Δ8 positions.

Most studies on LA biosynthesis have focused on bacterial metabolism, where there is evidence of a two-step lipoylation pathway involving the activity of the octanoyltransferase (LIP2) and lipoyl synthase (LIP1) enzymes (Cronan, 2016). In the first step, LIP2 transfers the octanoyl moiety from the octanoyl-acyl carrier protein (octanoyl-ACP) to the ε-amino group of highly conserved Lys residues close to the N-terminus of E2-PDH, establishing an amide link (Reed and Hackert, 1966). Subsequently, LIP1 generates the lipoyl cofactor by inserting sulfur atoms at C6 and C8 of the octanoyl chain in a reaction dependent on S-adenosyl methionine (SAM: Zhao et al., 2003). Unlike most cofactors, LA must be covalently bound to its cognate enzymes. Octanoyl-ACP is an intermediate in the fatty acid synthesis catalyzed by the type II plastidial fatty acid synthase (FAS), which depends on the acetyl-CoA synthesized by the lipoylated PDH. Therefore, both pathways are interdependent since E2-PDH lipoylation is essential for *de novo* fatty acid biosynthesis and vice versa. Moreover, plastidial E2-PDH

* Corresponding author.
E-mail address: ajmoreno@ig.csic.es (A.J. Moreno-Pérez).

https://doi.org/10.1016/j.jplph.2022.153730
Received 24 March 2022; Received in revised form 11 May 2022; Accepted 18 May 2022
Available online 22 May 2022

lipoylation is an essential process in plants, which are inviable without a functional form of that complex (Ewald et al., 2014b).

In addition to PDH, LA is an essential cofactor for the correct activity of other enzyme complexes that are involved in carbon metabolism in most eukaryotic and prokaryotic organisms. These complexes include 2-oxoglutarate dehydrogenase (OGDH), branched-chain 2-oxoacid dehydrogenase, acetoin dehydrogenase and the glycine cleavage system (known as glycine decarboxylase –GDC- in plants: Cronan, 2016). In *Escherichia coli* two pathways have been described that supply LA to these complexes: *de novo* LA biosynthesis achieved through lipoyl synthase and octanoyltransferase (called LIPA and LIPB, respectively: Cronan et al., 2016); and through the scavenging of free lipoate through lipoate protein ligase activity (LPLA: Zhao et al., 2003). Therefore, LIPB can be replaced by LPLA, whereas LIPA is essential for *E. coli* lipoylation (Zhao et al., 2003).

In higher eukaryotes, the LA biosynthetic pathways are not yet well defined. In plants, OGDH and GDC are located in the mitochondria, whereas PDH can be found within both mitochondria and plastids. These two organelles possess specific machinery for LA biosynthesis and protein lipoylation (Wada et al., 1997), and therefore, plants have both plastidial and mitochondrial forms of LIP1 and LIP2. In plant mitochondria, a LIP1-LIP2 *de novo* lipoylation pathway has been described (Wada et al., 2001; Yasuno and Wada, 1998), and while LPLA activity may also be involved in this process, its physiological role is not fully understood (Kang et al., 2007; Ewald et al., 2014a). By contrast, there is no evidence LPLA activity exists in plastids, and E2-PDH is thought to be lipoylated through specific LIP1 and LIP2 isoforms. LIP1 was reported in plastids from *Arabidopsis thaliana* (Yasuno and Wada, 2002), tomato (*Solanum lycopersicum*: Araya-Flores et al., 2020) and sunflower (*Helianthus annuus*: Martins-Noguerol et al., 2020). In Arabidopsis, both plastidial LIP1p and LIP2p are essential genes and therefore the double mutant is embryo lethal (Ewald et al., 2014b). The overexpression of sunflower plastidial LIP1 in Arabidopsis seeds altered the content of certain glycerolipid species (Martins-Noguerol et al., 2020). However, the involvement of plastidial LIP2 activity in plant fatty acid and lipid synthesis has not yet been characterized. The mitochondrial system of LA synthesis was recently studied in Arabidopsis plants, and the overexpression of sunflower mitochondrial *LIP1* and *LIP2* in Arabidopsis altered the host plant lipid composition, pointing to an involvement of sulfur metabolism (Martins-Noguerol et al., 2021). Furthermore, it was previously shown that suppressing LIP2 activity alters certain fatty acid species and increases the total fatty acids in seeds, suggesting the participation of LIP2 in the *de novo* fatty acid synthesis of Arabidopsis seeds (Martins-Noguerol et al., 2019).

This study is the last of a series studying the system of LA synthesis in sunflower. Here, two sunflower plastidial *LIP2* genes were identified, cloned and sequenced (*HaLIP2p1* and *HaLIP2p2*), and their expression in different plant tissues was studied. The phylogeny, structure, and catalytic mechanisms of both proteins was also analyzed *in silico*. Finally, after overexpression of *HaLIP2p1* and *HaLIP2p2* in *E. coli* and in Arabidopsis, the fatty acid and lipid content of both heterologous systems were analyzed, and the role of sunflower LIP2p in the metabolism of these molecules is discussed.

2. Materials and methods

2.1. Cloning of cDNAs encoding octanoyltransferases from H. annuus

The Arabidopsis plastidial octanoyltransferase (*At*LIP2p) protein sequence, encoded by the AT4G31050.1 gene and retrieved from public databases, was used to search for sunflower homologues in the sunflower genome database (Sunflower genome portal Heliagene - https://www.heliagene.org/: Badouin et al., 2017). Two cDNA molecules were selected, *HaLIP2p1* and *HaLIP2p2*, and specific PCR primers were designed to amplify both these genes, including their ATG and STOP codons (Table S1: primers were synthesized by Eurofins MWG Operon, Germany). The PCR fragments were purified and cloned into the pMBL-T Easy vector (Canvax, Spain), and the nucleotide sequences were confirmed by sequencing (Secugen, Spain). The confirmed sequences were deposited in GenBank under the accession numbers MT610110 (*HaLIP2p1*) and MT610111 (*HaLIP2p2*).

2.2. Protein sequence analysis

The protein sequences derived from the *Ha*LIP2p1 and *Ha*LIP2p2 genes were obtained using the BLASTp program (Camacho et al., 2009). These were aligned with homologous sequences and a phylogenetic analysis was performed using ClustalX v.2.0.10 software (Larkin et al., 2007) and MEGA6 software (Tamura et al., 2013). An *in silico* analysis of protein localization was carried out using the DeePLoc (Almagro Almagro Armenteros et al., 2017), TargetP V1.1 (Emanuelsson et al., 2007), iPSORT (Bannai et al., 2002) and Predotar (Small et al., 2004) applications. ClustalX v.2.0.10 and BioEdit (Hall, 1999) were used to study evolutionarily conserved residues through their alignment with homologous proteins from different phylogenetic groups: *Arabidopsis thaliana*, *Ricinus communis*, *Oryza sativa* and *Amborella trichopoda*. The location of theoretically critical residues and motifs involved in the catalytic activity of these novel proteins was deduced through their alignment with the crystal structure of octanoyltransferase from *Mycobacterium tuberculosis* (Protein Data Bank accession 1w66: Ma et al., 2006).

2.3. Modeling the three-dimensional structure of HaLIP2p and molecular docking

Homology modeling was performed using the Swiss Model server (Schwede et al., 2003; http://swissmodel.expasy.org/) and the *M. tuberculosis* LIPB X-ray structure as a template (*Mt*LIPB: Ma et al., 2006). The UCSF Chimera program (Pettersen et al., 2004) was used to visualize the model. Molecular docking was performed using the SwissDock server (Grosdidier et al., 2011a and 2011b) with octanoic acid as a substrate (ZINC01530416). The docking model was then visualized and analyzed with the UCSF Chimera program.

2.4. Real-time quantitative PCR (RT-qPCR)

The expression of *HaLIP2p1* and *HaLIP2p2* was analyzed by RT-qPCR using sunflower cDNAs from developing seeds (16, 20, 25 and 30 days after anthesis – DAA), roots, stems, cotyledons and leaves. A CFX96 TM real-time PCR detection system (Bio-Rad) was used to perform the reactions with SYBR Green I (QuantiTec SYBR Green PCR Kit: Qiagen, Crawley, UK) and specific primer pairs (HaLIP2p1qpcr-F/HaLIP2p1qpcr-R for *HaLIP2p1* and HaLIP2p2qpcr-F/HaLIP2p2qpcr-R for *HaLIP2p2*: Table S1) over 40 PCR cycles: 94 °C for 30 s, 57 °C for 30 s and 72 °C for 1 min. The Livak $2^{\Delta\Delta Ct}$ method (Livak and Schmittgen, 2001) were used to calculate their expression normalized to the sunflower housekeeping gene actin (*Ha*ACT, GenBank Accession No. FJ487620, *Ha*Actin-qpcr-F4 and *Ha*Actin-qpcr-R4 primers: Table S1).

2.5. Expression and purification of recombinant proteins in Escherichia coli

The sequences corresponding to the mature *Ha*LIP2p1 and *Ha*LIP2p2 were cloned into the pQE-80L expression vector (Qiagen, Germany) using the *BamHI/XbaI* and *BamHI/PstI*, restriction sites, respectively, allowing $(His)_6$-fusion proteins to be produced for purification. The specific primer pairs designed for this cloning were: HaLIP2p1-B-BamHI-F/HaLIP2p1-PstI-R for *Ha*LIP2p1; and HaLIP2p2-B-BamHI-F/HaLIP2p2-PstI-R for *Ha*LIP2p2 (Table S1). The fidelity of the pQE-80L::*HaLIP2p1* and pQE-80L::*HaLIP2p2* constructs was confirmed by sequencing, and they were then expressed in *E. coli* XL1-Blue cells grown at 37 °C with shaking in LB media (1% Bacto Tryptone, 0.5% yeast

extract, 1% NaCl [pH 7]), and containing 50 μg/mL ampicillin. Isopropyl b-D-1-thiogalactopyranoside (IPTG) was added to a final concentration of 0.5 mM to induce protein production when the cultures reached an OD $_{600nm}$ value of 0.4. After 4 h growth, the cells were harvested by centrifugation (3000×*g* for 20 min), resuspended in Binding Buffer (20 mM sodium phosphate [pH 7.4], 500 mM NaCl, 20 mM imidazole) and disrupted with 15 cycles of sonication (70° amplitude during 10 s pulses with 10 s intervals for cooling on ice). Soluble fractions for protein purification were obtained by centrifugation at 2000×*g* at 4 °C for 30 min and the recombinant proteins were purified using the HisSpinTrap Kit (GE Healthcare, UK), following the manufacturer's instructions. Protein-enriched eluates were monitored by SDS-PAGE and the $(His)_6$-tagged recombinant proteins were then visualized in Western Blots (see Martins-Noguerol et al., 2020).

2.6. Fatty acid analysis of transgenic Escherichia coli

Cultures of the *Escherichia coli* XL1-Blue harboring pQE-80L::*HaLIP2p1*, pQE-80L::*HaLIP2p2* or an empty pQE-80L vector were grown and induced as described above. The cells were harvested by centrifugation (3000×*g* for 20 min) and washed twice with distilled water. Total lipids from he cultures were methylated using a methylation mixture containing methanol/toluene/sulfuric acid (88:10:2, v/v/v) and heated for 1h at 80 °C (Garcés and Mancha, 1993). Heptadecanoic acid (17:0) was added as an internal standard. The total fatty acid methyl esters (FAMES) were extracted by adding 1 mL of heptane and the upper phase was then washed with 2 mL Na_2SO_4 (6.7%) in a new tube. The resulting fraction was evaporated under nitrogen gas and the methyl esters obtained were resuspended in 200 μL heptane. Gas chromatography (GC) analysis were performed as described in Martins-Noguerol et al. (2021).

2.7. Generation of transgenic Arabidopsis thaliana plants

The mature sequence of the *HaLIP2p1* gene was cloned into a pBIN19-35S binary vector that contains the 35S promoter from cauliflower mosaic virus (CaMV). The sequence flanked by the *Bam*HI and *Pst*I restriction sites was obtained in PCR reactions with specific primers (HaLIP2p1-BamHI-F/HaLIP2p1-PstI-R: Table S1) and then cloned into pBIN19-35S using the respective restriction sites. The CAMV-35S–F and pBIN19-R primers were used for PCR screening of the construct (Table S1), which was subsequently confirmed by sequencing. The construct was used to transform competent *Agrobacterium tumefaciens* GV3101 cells, which were used to generated transgenic Arabidopsis lines were by floral dipping (Sayanova et al., 2006). *A. thaliana* Columbia (Col-0) ecotype plants were grown in a growth chamber under a controlled environment (22 °C day/20 °C night, 60% humidity, 16 h photoperiod at 250 μmol m^{-2} s^{-1}) and first generations seeds from the transformed plants were selected by germination in MS medium supplemented with 50 μg/mL kanamycin (Harrison et al., 2006). Gene insertion was confirmed by PCR using Arabidopsis gDNA, and the expression of *HaLIP2p1* in transgenic plants was confirmed by RNA extraction, cDNA synthesis and PCR. Third generation seeds from confirmed transgenic *A. thaliana* plants were used for the lipid analysis.

2.8. Fatty acid analysis of transgenic arabidopsis seeds

Total lipids were extracted from three replicates of mature seeds (10 mg) from wild-type (WT) Col-0 and third-generation transgenic plants overexpressing *HaLIP2p1*. The fatty acid composition of the total lipid seed extract was determined as described previously (Martins-Noguerol et al., 2020). The total lipids were extracted using glass beads in a Precellys homogenizer (6000 rpm for 30 s, 3 cycles: Precellys 24, Ozyme), and then 1 mL hexane:isopropanol (2:1) was added. After solvent evaporation, the lipids were resuspended in chloroform:methanol (1:1) and methylated with 5 μL of tetramethylammonium hydroxide (TMAH) solution (Sigma-Aldrich). Finally, 50 μL of decane was used to stop the reaction and 20 μL of the upper phase was used to analyze the FAMEs by GC.

2.9. Lipidomic analysis

For lipidomic studies, lipids were extracted from ice-dried Arabidopsis seeds (20 mg) as described previously (Martins-Noguerol et al., 2019). Once the lipids were extracted, the solvent was evaporated in an atmosphere of nitrogen and the lipids were solubilized in 200 μL isopropanol. The samples were diluted four times and analyzed by ultra-high performance liquid chromatography coupled to quadrupole-time of flight (QToF) mass spectrometry (UHPLC-HRMS2), performed following the protocol described by Ulmer et al. (2017) with some modifications. LC was performed on a HPLC 1290 (Agilent Technologies) and the lipid species were separated on a C18 Hypersil Gold column (100 × 2.1 mm, 1.9 μm: Thermofisher), following the temperature and gradient solvent conditions described in Martins-Noguerol et al. (2019). LC-electrospray ionization (ESI)-HRMS2 analysis was performed by coupling the LC system to a hybrid QToF high definition mass spectrometer (Agilent 6538: Agilent Technologies) equipped with a dual ESI source. The parameters were controlled using MassHunter B.07 software and the chromatogram was built as described in Martins-Noguerol et al. (2020). The peaks were annotated using two different databases: lipid Match (Koelmel et al., 2017) and lipid Blast (Kind et al., 2013).

2.10. Statistical analysis

Statistical analysis was carried out using IBM SPSS v. 24.0 software (IBM Corp., Armonk, N.Y., USA). The data were tested for normality (Kolmogorov-Smirnov test) and homogeneity of variance (Levene test), and a one-way analysis of variance (ANOVA) was performed determining the significant differences with a Tukey test. The data from the lipidomic analysis were analyzed using Metaboanalyst v4.0 (Chong et al., 2019) and performing a multivariate analysis. A principal component analysis (PCA) was performed to study the differences in the lipid profiles among the different genotypes. Finally, an agglomerative analysis was carried out to obtain hierarchical clusters, which were represented together with heatmaps in which the cells represent the concentration of each lipid species.

3. Results

3.1. Cloning and sequence analysis of two lipoyl octanoyltransferases from sunflower

Two coding sequences were identified within the sunflower genome database (Heliagene, Badouin et al., 2017) based on their homology to the Arabidopsis LIP2p gene (At4g31050.1), located on chromosome 9 (*HaLIP2p1;* HanXRQChr09g0268371) and chromosome 5 (*HaLIP2p2;* HanXRQChr05g0141551). Using these sequences, PCR products of 874 bp (*HaLIP2p1*) and 873 bp (*HaLIP2p2*) were amplified from 25 DAA sunflower seed cDNA, and the protein sequences encoded by these cDNAs contained 283 (*Ha*LIP2p1) and 290 (*Ha*LIP2p2) residues. When these genes were launched into location predictors (DeePLoc: Almagro Almagro Armenteros et al., 2017) they were both clearly classified as plastidial proteins (Figs. S1 and S2). The plastid transit peptide was located in the N-terminus of the proteins, Arg52 and Arg46, representing the first residues in the mature *Ha*LIP2p1 and *Ha*LIP2p2 proteins, respectively (Fig. S4). The mature *Ha*LIP2p1 had 231 aa, with a theoretical molecular weight of 25.99 kDa and a pI of 5.45. The mature *Ha*LIP2p2 contained 247 aa, with a theoretical molecular weight of 27.84 and a pI of 5.82. In both the chloroplast signal peptides there is a predominance of Ser, Pro and Thr residues. A phylogenetic analysis was performed with the predicted amino acid sequences of both the novel sunflower proteins, *Ha*LIP2p1 and *Ha*LIP2p2, along with other known

homologous plant proteins (Fig. 1). The dendrogram showed that both these proteins are close to those from *Cynara cardunculus* and *Lactuca sativa*, forming a group corresponding to Asteraceae family within the dicot subtree. In order to study the conserved and catalytic residues in the sequence of sunflower proteins, their deduced amino acid sequences were aligned with their homologues from different phylogenetic groups (*Arabidopsis thaliana*, *Ricinus communis*, *Oryza sativa* and *Amborella trichopoda*), highlighting the conserved residues and domains in the octanoyltransferases enzymes (Fig. S4).

Catalytic residues (indicated in the alignment: Fig. S4) were identified in accordance with the alignment of both sunflower protein sequences together with the crystalized *Mycobacterium tuberculosis* octanoyltransferase sequence (*Mt*LIPB: Ma et al., 2006). Two invariant residues (Cys176 and Lys142 in *M. tuberculosis*) have been postulated to act as acid-base catalysts, with the Cys residue binding covalently to the substrate through a thioesther bond. These residues correspond to Cys229 and Lys195 in *Ha*LIP2p1, and Cys223 and Lys189 in *Ha*LIP2p2, and these Cys residues constitute part of a highly conserved PCG motif (Pro228-Cys-Gly230 in *Ha*LIP2p1, and Pro222-Cys-Gly224 in *Ha*LIP2p2). Homologous conserved aromatic residues that interact with the substrate in *Mt*LIPB (Tyr22, His49, His83 and Tyr91) were found in the sunflower proteins: Trp72, His99, His137 and Tyr145 in *Ha*LIP2p1; Trp66 His93, His131 and Tyr139 in *Ha*LIP2p2. Several conserved *Mt*LIPB Gly residues (Gly77, Gly78, Gly147 and Gly158) that are involved in cavity formation for the substrate interaction were also detected in the *Ha*LIP2p1 (Gly131, Gly132, Gly200 and Gly211) and

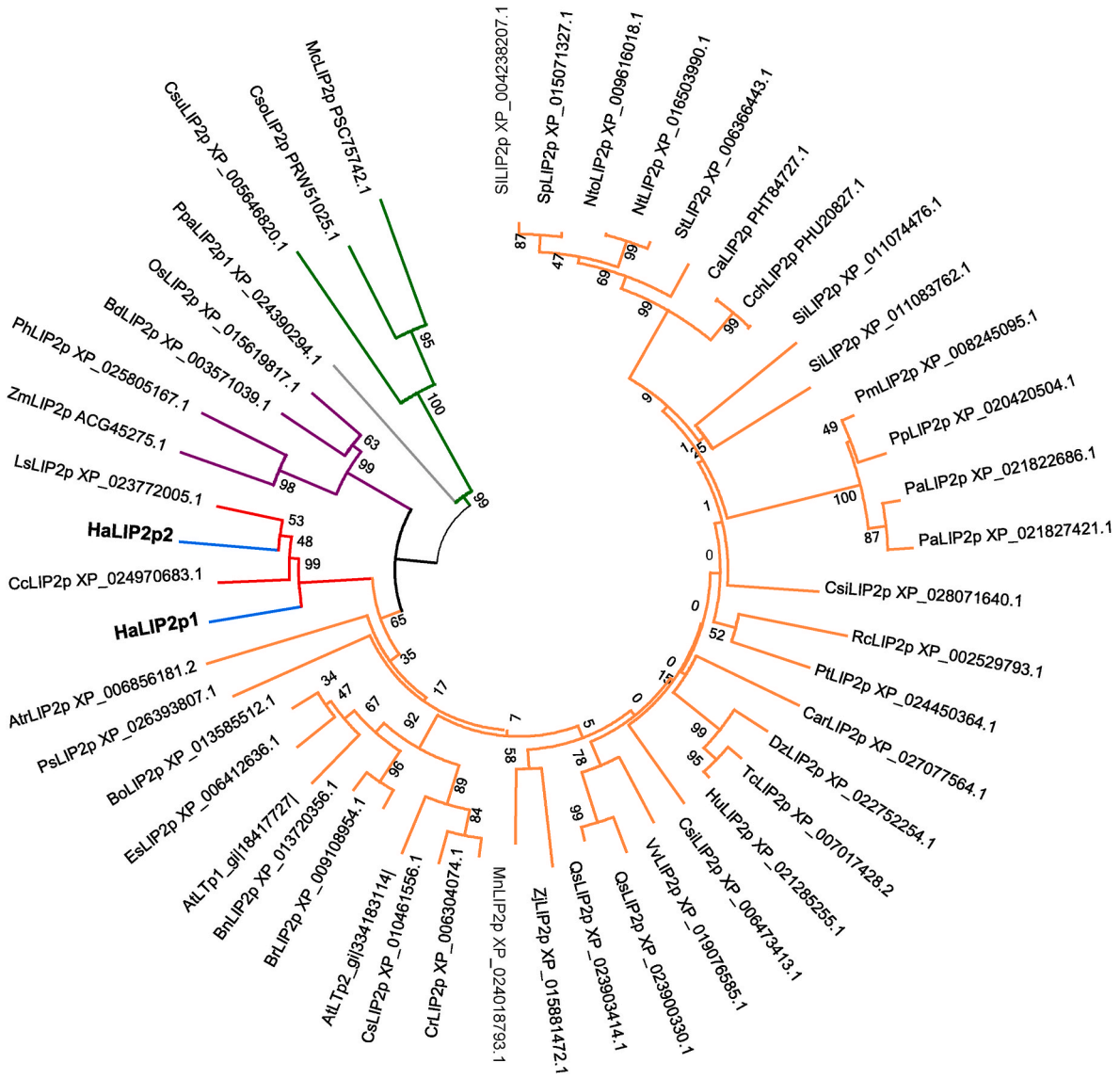

Fig. 1. Phylogenetic tree of plant plastidial octanoyltransferases. Plant species included in the phylogenetic tree are: *At. *Arabidopsis thaliana*; Atr. *Amborella trichopoda*; Bd. *Brachypodium dystachyon*; Bn. *Brassica napus*; Bo. *Brassica oleraceae*; Br. *Brassica rapa*; Ca. *Capsicum annuum*; Car. *Coffea arabica*; Cc. *Cynara cardunculus*; Cch. *Capsicum chinense*; Cr. *Capsella rubella*; Cs. *Camelisa sativa*; Csi. *Camellia sinensis*; Csi. *Citrus sinensis*; Dz. *Durio zibethinus*; Es. *Eutrema salsugineum*; Hu. *Herratia umbratica*; Ls. *Lactuca sativa*; Mn. *Morus notabilis*; Nt. *Nicotiana tabacum*; Nto. *Nicotiana tomentosiformis*; Os. *Oryza sativa*; Pa. *Prunus avium*; Ph. *Panicum hallii*; Pm. *Prunus mume*; Pp. *Prunus persica*; Ppa. *Physcomistrella patens*; Ps. *Papaver somniferum*; Pt. *Populus trichocarpa*; Qs. *Quercus suber*; Rc. *Ricinus comunis*; Si. *Sesamum indicum*; Sl. *Solanum lycopersicum*; Sp. *Solanum pennellii*; St. *Solanum tuberosum*; Tc. *Theobroma cacao*; Vv. *Vitis vinifera*; Zj. *Ziziphus jujuba*; Zm. *Zea mays*; Green algae species were included an as outgroup to root the tree (in green): Cso. *Chlorella sorokiniana*; Csu. *Coccomyxa subellipsoidea*; Mc. *Micractinium conductrix*. The purple subtree represents monocots. *Ha*LIP1p1 and *Ha*LIP1p2 (in blue) are included in the *Asteraceae* family (in red) within the dicot group (in orange). The numbers in the tree represent the bootstrap values for each tree node from the phylogenetic analysis.

*Sequences coding for characterized enzymes with octanoyltransferase activity experimental evidence. (For interpretation of the references to colour in this figure legend, the reader is referred to the Web version of this article.)

*Ha*LIP2p2 sequences (Gly125, Gly126, Gly194 and Gly205). Finally, *Mt*LIPB has been said to possess a predominance of positively charged residues (Arg58, Arg79, Arg130 and Arg149) in the substrate access site, residues that are less well conserved in the sunflower given that several changes were found, although some of the positively charged residues were preserved: Ala108, Leu186 and Arg202 in *Ha*LIP2p1; and Ala102, Leu180 and Arg196 in *Ha*LIP2p2.

3.2. Prediction and docking of the tertiary structure model

In the absence of a crystal structures for plant octanoyltransferases, the *Mt*LIPB X-ray structure was used as template to model the tertiary structures of *Ha*LIP2p1 and *Ha*LIP2p2. *Mt*LIPB shared 38.16% sequence similarity with *Ha*LIP2p1, and 35.75% with *Ha*LIP2p2. Both sunflower proteins shared 67.70% of identity and as such, the model generated was quite similar for both sequences (Fig. S5). The overall predicted structure for both proteins consisted of a monomer whose secondary structure was formed by several β strands forming a core, and several α helices surrounding this core. In *Ha*LIP2p1, 8 α helix and 9 β strands were found, as opposed to 9 α helix and 8 β strands in *Ha*LIP2p2. The distribution of the secondary elements in the tertiary structure was very similar to that in the template, and a gap in the core was formed by two β-sheets where it is presumed that the substrate interacts. Several α-helices protrude around the β-strands. In *Ha*LIP2p1, the large β sheet is forming by six β strands (β1-β2-β6-β7-β8-β9) and the small sheet is made up of three (β3-β4-β5). In *Ha*LIP2p2, the large β-sheet also consisted of six β strands (β1-β2-β5-β6-β7-β8), although only two β strands were considered to form the minor β sheet (β3-β4). Despite these differences, the 3D view of molecular surface was essentially the same for both these proteins (Fig. S5).

The *Ha*LIP2p docking model was generated using octanoic acid as a substrate (Fig. S6). Octanoic acid was positioned in the gap formed by the two β sheets, which is visible in the molecular surface model (Fig. S6A). The carboxyl group of octanoic acid was close to the Cys residue (Figs. S6B–C) with which it presumably interacts. In our docking model the conserved Lys was also located close to the Cys in the structure core. Moreover, all the aforementioned residues that participated in the substrate interaction or gap formation were found to be close to the active site of the enzyme.

3.3. HaLIP2p1 and HaLIP2p2 tissue distribution

The expression of *HaLIP2p1* and *HaLIP2p2* was studied by RT-qPCR in developing seeds and vegetative tissues. Both genes were expressed in all the tissues analyzed, although less *HaLIP2p2* accumulated than *HaLIP2p1,* the latter representing the predominant isoform in sunflower (Fig. 2). These transcripts were temporally regulated during embryo development, with the strongest expression of the *HaLIP2p1* gene in developing seeds evident at 18 DAA. Moreover, the main expression of this gene in the vegetative tissues was detected in leaves.

3.4. Fatty acid analysis of E. coli expressing the HaLIP1p1 and HaLIP1p2 enzymes

Both sunflower octanoyltransferases were expressed in *E. coli* using the pQE-80L vector (pQE-80L::*HaLIP2p1* and pQE-80L::*HaLIP2p2*) and both soluble proteins were purified from cell extracts (Fig. S3). The involvement of *HaLIP1p1 and HaLIP1p2* in fatty acid biosynthesis was assessed by analyzing the fatty acids in the transgenic bacteria (Table 1). The overexpression of both sunflower octanoyltransferases altered the fatty acid profile and when *HaLIP2p1* was overexpressed, there was a significant decrease of $16{:}1^{\Delta 9}$ and 16:0, and an increase of 14:0 and $18{:}1^{\Delta 11}$ fatty acid species relative to the control. The overexpression of *HaLIP2p2* produced a significant decrease in the unsaturated $16{:}1^{\Delta 9}$ and $18{:}1^{\Delta 11}$ fatty acids. In terms of the unsaturated/saturated ratio, there were differences in the cultures overexpressing *HaLIP2p1* in which that ratio decreased. Finally, a decrease in the total fatty acid content was observed in the cultures when *HaLIP2p1* and *HaLIP2p2* were overexpressed (Table 1).

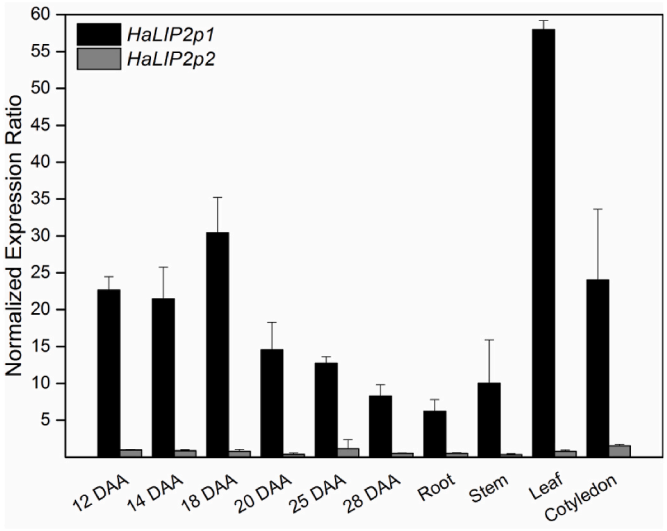

Fig. 2. The expression of the plastidial octanoyltransferase genes *HaLIP2p1* and *HaLIP2p2* in *H. annuus* normalized to the sunflower housekeeping gene actin (*HaACT*): DAF, days after flowering. The data represent the mean ± SD values of three independent biological samples with three technical replicates from each one in different experiments.

Table 1
Fatty acid composition (%) of *E. coli* harbouring different constructs: empty pQE-80L, pQE-80L::*HaLIP2p1* or pQE-80L::*HaLIP2p2*. The cultures were induced with 0.5 mM IPTG, and the data represent the average and standard deviation of three independent replicates.

	pQE-80L	pQE-80L::*HaLIP2p1*	pQE-80L::*HaLIP2p2*
14:0	3.45 ± 0.21[a]	4.00 ± 0.21[b]	3.79 ± 0.12[ab]
16:0	43.58 ± 0.89[a]	40.21 ± 0.26[b]	43.44 ± 1.70[a]
$16{:}1^{\Delta 9}$	21.65 ± 0.27[a]	18.20 ± 0.30[b]	19.99 ± 0.56**c**
17:0Δ[A]	7.97 ± 0.41[a]	8.85 ± 0.34[a]	8.40 ± 0.76[a]
18:0	0.79 ± 0.13[a]	0.93 ± 0.19[a]	2.58 ± 2.41[a]
$18{:}1^{\Delta 11}$	22.04 ± 0.38[a]	27.15 ± 0.62[b]	20.20 ± 0.76[c]
19:0Δ[A]	0.52 ± 0.32[a]	0.66 ± 0.17[a]	2.61 ± 3.77[a]
SFA[B]	47.82 ± 0.81[a]	45.14 ± 0.09[b]	48.80 ± 2.81[ab]
UFA[C]	52.18 ± 0.81[a]	54.86 ± 0.09[b]	51.20 ± 2.81[ab]
UFA/SFA	1.09 ± 0.01[a]	1.22 ± 0.02[b]	1.05 ± 0.01[ab]
mg FAs/unit of ABS_{600nm}	0.39 ± 0.01[a]	0.24 ± 0.01[b]	0.25 ± 0.03[b]

*Significant differences ($p < 0.05$).
[d] 19:0Δ.
[a] Cyclopropanes C17 and 19 derived from C16:1 and 18:1, respectively.
[b] Saturated fatty acids: 14:0 + 16:0 + 18:0.
[c] Unsaturated fatty acids and derivatives: $16{:}1^{\Delta 9}$ + 17:0Δ + $18{:}1^{\Delta 11}$.

3.5. Fatty acid profile of transgenic Arabidopsis thaliana seeds

The third generation of mature transgenic seeds from confirmed transgenic *A. thaliana* plants overexpressing *HaLIP2p1* were harvested. The overexpression of *HaLIP2p1* did not modify plant growth, displaying a similar phenotype to WT plants (Fig. S7). No significant changes were observed in the fatty acid profile of transgenic seeds relative to the control lines (Table 2).

Table 2
Fatty acid composition (mol %) of transgenic Arabidopsis seeds overexpressing *HaLIP2p1*. The data represent the average and SD of three independent transgenic Arabidopsis lines in different experiments.

	WT Col-0	*Ha*LIP2p1
16:0	7.69 ± 0.05	7.74 ± 0.67
16:1$^{\Delta 9}$	0.21 ± 0.04	0.17 ± 0.05
18:0	3.46 ± 0.11	3.52 ± 0.32
18:1$^{\Delta 9}$	17.35 ± 0.07	17.75 ± 0.29
18:1$^{\Delta 11}$	0.09 ± 0.03	0.09 ± 0.01
18:2$^{\Delta 9\Delta 12}$	27.79 ± 0.25	28.16 ± 0.30
18:3$^{\Delta 9\Delta 12\Delta 15}$	16.04 ± 0.04	15.72 ± 0.19
20:0	2.01 ± 0.05	2.04 ± 0.04
20:1$^{\Delta 11}$	21.33 ± 0.18	20.86 ± 0.26
20:1$^{\Delta 13}$	1.70 ± 0.01	1.75 ± 0.02
20:2$^{\Delta 9\Delta 12}$	0.29 ± 0.02	0.29 ± 0.03
22:0	0.23 ± 0.01	0.18 ± 0.02
22:1$^{\Delta 13}$	1.67 ± 0.05	1.62 ± 0.03
24:0	0.14 ± 0.08	0.10 ± 0.02
SFA[a]	13.53 ± 0.02	13.58 ± 0.95
UFA[b]	86.47 ± 0.02	86.42 ± 0.95
UFA/SFA	6.39 ± 0.01	6.39 ± 0.50

[a] Saturated fatty acids: 16:0 + 18:0 + 20:0 + 22:0 + 24:0.
[b] Unsaturated fatty acids and derivatives: 16:1$^{\Delta 9}$ + 18:1Δ9 +18:1Δ11 + 18:2Δ9Δ12+18:3Δ9Δ12Δ15+20:1Δ11+20:1Δ13+20:2Δ9Δ12+22:1Δ13.

3.6. Lipidomics in transgenic Arabidopsis thaliana seeds

A comparative lipidomics analysis between WT and transgenic *HaLIP2p1* Arabidopsis seeds identified significant differences in the content of 46 of the 70 annotated lipids studied ($p < 0.05$). Subsequently, a PCA was carried out to determine the experimental variation, clustering different genotypes in score plots that provide an overview of the differences in seed oil composition among the WT and transgenic lines. The accumulated variance explained by principal component 1 (PC1) was 69.2%, while that explained by PC2 reached 26.2% (Fig. S8). Agglomerative hierarchical clustering was performed and the result was showed as a heatmap, in which the 25 lipids displaying the most significant differences in t-tests were shown (Fig. 3). Clear changes in the content of several triacylglycerol (TAG) species were evident and as a result, the 25 most abundant lipids were selected and significant differences were identified (Fig. 4). *HaLIP2p1* expression in Arabidopsis seeds produced an increase in TAG 54:7 (18:2/18:2/18:3), 56:3 (18:1/18:1/20:1), 54:4 (18:1/18:1/18:2), 58:5 (18:2/20:1/20:2), 58:4 (18:2/20:1/20:1), 58:3 (18:1/20:1/20:1), 54:8 (18:2/18:3/18:3), 58:6 (18:3/20:1/20:2), 54:2 (16:0/18:1/20:1), 52:2 (16:0/18:1/18:1), 52:6 (16:0/18:3/18:3) and 56:2 (18:0/18:1/20:1) and PC 36:5 (18:2/18:2). By contrast, TAG species that decreased were 56:6 (18:2/18:3/20:1), 56:5 (18:2/18:2/20:1), 56:7 (18:2/18:3/20:2), 54:6 (18:1/18:2/18:3) and 52:4 (16:0/18:2/18:2).

4. Discussion

Plastidial octanoyltransferase and lipoyl synthase are key enzymes involved in LA biosynthesis in this organelle. LA is necessary for the activity of the plastidial PDH complex, which catalyzes the oxidative decarboxylation of pyruvate to acetyl-CoA, the source of carbon for *de novo* fatty acid biosynthesis. Studies of metabolic flux have shown that carbon imported into plastids and used for fatty acid synthesis comes from carbohydrates degraded through the cytosolic glycolytic pathway. The glycolytic metabolites imported by plastids are typically glycose-6-phosphate, phosphoenolpyruvate and pyruvate, in proportions that depend on the specific plant species (Schwender et al., 2003; Alonso et al., 2007). The degradation of these metabolites continues within the plastid, which has endogenous glycolytic capacity, and they are all transformed into pyruvate. Thus, the production of the acetyl-CoA required for fatty acid synthesis relies on the plastidial PDH complex, which should contain its LA co-factor, with both these events related and essential for the correct development of plant cells, and for the production of reserve TAGs. Therefore, better understanding the plastidial

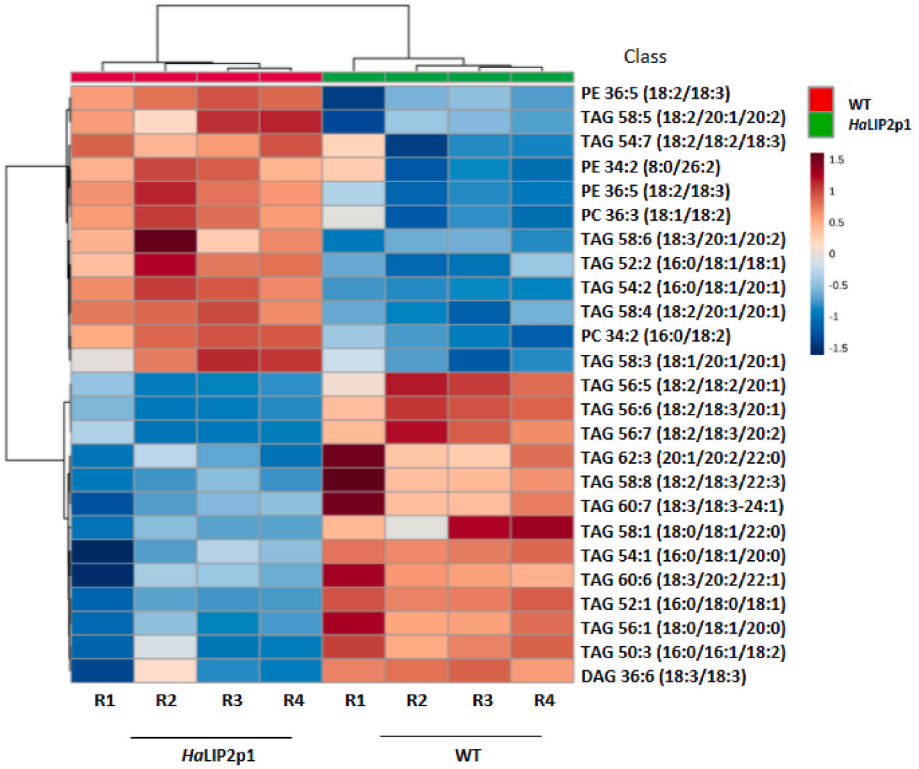

Fig. 3. Dendrogram and heat map of different lipid species (on the right), comparing wild-type seeds (WT; in red) with transgenic seeds overexpressing *Ha*LIP2p1 (in green). (For interpretation of the references to colour in this figure legend, the reader is referred to the Web version of this article.)

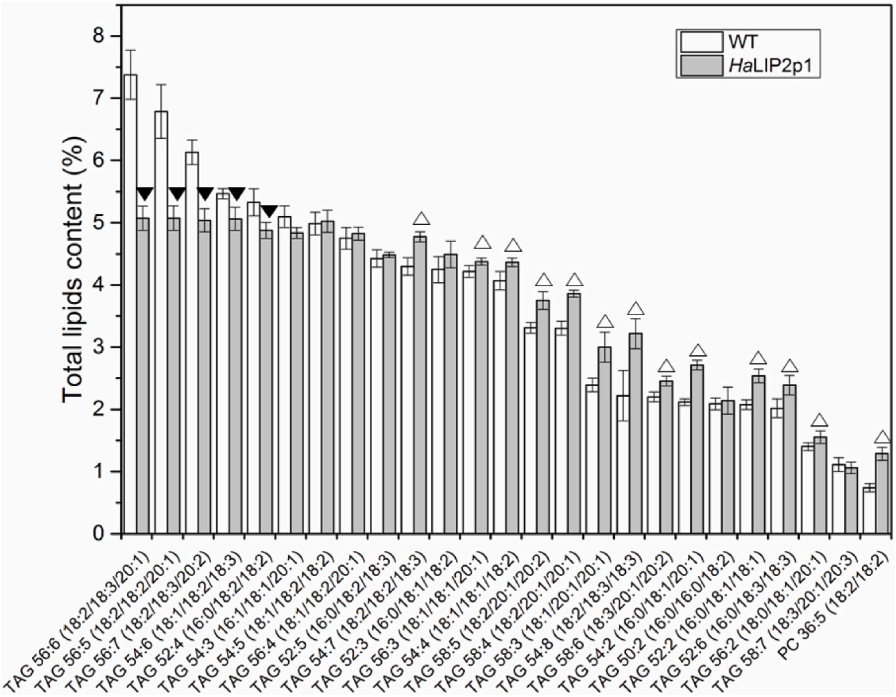

Fig. 4. Representative differences in the TAG and glycerolipid species found in mature wild-type Arabidopsis seeds (WT, white columns) and mature transgenic Arabidopsis seeds that overexpress *Ha*LIP2p1 (grey). The data are the averages ± SD of three different transgenic Arabidopsis lines in different experiments, where △▼ reflect significant differences at the 0.05 level.

lipoylation pathway is critical to design approaches that modify the lipid composition of sunflower plants.

In the present study, two sunflower seed octanoyltransferase genes, *HaLIP2p1* and *HaLIP2p2,* were cloned and studied. These *LIP2* encoded proteins shared 67.70% identity, with the main differences in the N-terminal transit signal peptide. Indeed, the presence of these N-terminal signal peptides suggests a high likelihood of a plastidial location. In both cases the N-terminal sequences were enriched in Pro, Ser and Thr amino acids, and these residues were described as typical amino acids in plastid signal peptides (Zhang and Glaser, 2002; von Heijne et al., 1989). Previous studies showed that sunflower plastidial enzymes also accumulate these phosphorylation motifs (e.g., *Ha*FatA, *Ha*FAD7, *Ha*KASIII, *Ha*HAD1-2 and *Ha*LIP1s: Serrano-Vega et al., 2005; Venegas-Calerón et al., 2006; González-Mellado et al., 2010; González-Thuillier et al., 2016; Martins-Noguerol et al., 2020), pointing to similar processes of protein maturation for the products of all these genes.

Phylogenetic analysis points to a duplication as the potential origin of these two sequences, a common origin that is presumable related to the hybrid origin of the Helianthus genus (Giordani et al., 2014). The localization of the two LIP2p sunflower genes on different chromosomes supports this hypothesis, as does the close proximity of the *Ha*LIP2p1 and *Ha*LIP2p2 proteins to other members of the Asteraceaea family, such as *Cynara cardunculus* and *Lactuca sativa*. The alignment of both LIP2p proteins with homologous sequences from other plant species identified highly conserved catalytic residues (Ma et al., 2006) and motifs, indicating the little variation among octanoyltransferases during evolution. In the novel sunflower *Ha*LIP1p1 and *Ha*LIP2p2, these two catalytic residues correspond to Cys229/Lys195 and Cys223/Lys189, respectively, the Cys residue forming part of the conserved PCG motif in both these sunflower proteins (Pro228-Cys229-Gly230 in *Ha*LIP2p1; Pro222-Cys223-Gly224 in *Ha*LIP2p2). Besides these previously described residues, other conserved amino acids involved in substrate interaction and accommodation were identified in the crystalized *Mt*LIPB protein (Ma et al., 2006). Homologous amino acids to these key residues were found in both sunflower sequences, confirming the conservation of these critical residues during octanoyltransferase evolution.

Octanoyltransferases act as Cys/Lys acyltransferases, whereby the Cys residue interacts with the carboxyl group of the octanoyl group from octanoyl-ACP and an acyl-thioester intermediate is formed (Ma et al., 2006). Thus, the octanoyl group is transferred to a lipoyl domain of apo-proteins (Zhao et al., 2005). Moreover, the involvement of the conserved Lys has been demonstrated in the catalytic activity of *Mt*LIPB (Ma et al., 2006) and when no substrate is available, this Lys is close to the sulfhydryl group of the Cys residue, suggesting a hydrogen bond may form between this Lys-Cys. This could generate a nucleophile group for acyltransferase activity. Furthermore, this Lys has been suggested to participate in the activation of the octanoyl chain for thioester octanoyl-Cys formation (Ma et al., 2006). The docking model obtaining for *Ha*LIP2p suggests it possesses a mechanism analogous to that described previously, with octanoic acid located in the gap, with the aliphatic chains inbound and the carboxyl group very close to the Cys with which it would interact through a thioester bond. Moreover, the Cys and Lys residues stay close together. This mimics the proposed model for *Mt*LIPB, where Lys forms part of a β-strand (as also occurs in *Ha*LIP2p1 and *Ha*LIP2p2) close to the Cys. Furthermore, these observations were also described in *E. coli* LIPB, where the octanoyltranferase reaction was proposed to take place through the formation of an acyl-thioester intermediate between the octanoyl chain and the Cys from LIPB (Zhao et al., 2005). Thus, the structure and docking data from both sunflower plastidial LIP2 suggest an identical activity.

Gene expression suggests that none of these enzymes are tissue specific. Two octanoyltransferases were identified in *A. thaliana* (*At*LIP2p and *At*LIP2p2: Ewald et al., 2014b), and although *At*LIP2p1 is the most strongly expressed in leaves and roots, *At*LIP2p2 dominates in siliques and flowers. Nevertheless, both were seen to be redundant and the expression of at least one of them was essential for plant development (Ewald et al., 2014b). In sunflower, the prevalence of *HaLIP2p1* expression, in contrast with the relatively low levels of *HaLIP2p2* (Fig. 2), suggests that *Ha*LIP2p1 is the main octanoyltransferase involved in the attachment of octanoyl chain to plastidial E2-PDH. Moreover, when both enzymes were overexpressed in *E. coli*, different changes in fatty acid composition were detected. In the biosynthesis of

bacterial and plant plastid/chloroplast fatty acids, PDH catalyzes the production of acetyl-CoA, the source of carbon necessary for this anabolic process. In this pathway, β-ketoacyl-ACP synthase (FABB) uses octanoic acid to provide decanoic acid for further fatty acid synthesis. In this sense, competition for the octanoyl-ACP substrate could exist between LIPB and FABB, and in this context, an excess of octanoyltransferase activity (due to *HaLIP2p1* and *HaLIP2p2* overexpression) could drive the retention of more octanoate by this enzyme. This would lead to a depletion in octanoic acid for acyl elongation and therefore, a decrease in fatty acid biosynthesis. This would be coherent with the decrease in the absolute amounts of fatty acids that *Ha*LIP2p genes produce in bacteria when overexpressed (Table 1). Moreover, it is important to consider that *E. coli* has other lipoylated proteins, such as 2-oxoglutarate dehydrogenase (2OGDH) and protein H of the glycine cleavage system (Vanden Vanden Boom et al., 1991; Wilson et al., 1993). Hence, the distinct impact on fatty acid profiles could be related to the putative specificity of sunflower LIP2 in bacteria.

The *HaLIP2p1* gene was selected instead of *HaLIP2p2* to obtain overexpressing Arabidopsis plants because it is the most strongly expressed octanoyltransferase gene in vegetative tissues and developing sunflower seeds. Seed germination rates and plant development were not affected in Arabidopsis transgenic plants (Fig. S7), and nor was the seed fatty acid composition of the mutant line (Table 2). In Arabidopsis, plastidial PDH complex supplies acetyl-CoA for *de novo* fatty acids biosynthesis and β-ketoacyl-ACP synthase I (KAS I) is the responsible for fatty acid elongation from octanoic acid (C8:0) up to palmitic acid (C16:0: Wu and Xue, 2010). As we hypothesized for bacteria, a potential competition between KAS I and LIP2p proteins is present within plastids. *HaLIP2p1* overexpression could produce an excess of octanoyltransferase activity, leading to a depletion of octanoyl-ACP in Arabidopsis plastids. Accordingly, a reduced availability of octanoyl-ACP for KAS I activity will lead to a decrease in fatty acid synthesis. Previously, Arabidopsis mutants with low KAS I and KAS III activities were seen to have reduced fatty acids synthesis (Wu and Xue, 2010; Takami et al., 2010). In order to clarify the role of LIP2p during fatty acid synthesis, a relatively complete lipidomics analysis in transgenic seeds was carried out. This study revealed different lipid profiles in both transgenic and WT seeds. The PCA analysis separated the data from both genotypes indicating that the overexpression of *HaLIP2p1* had consequences on lipid biosynthesis. Furthermore, the heatmap identified glycerolipid species, mainly TAGs, with significant alterations in their content due to *HaLIP2p1* overexpression. Some of the TAG whose content changed coincided with the most abundant TAG species in Arabidopsis seeds (e.g. TAG 56:6 or TAG 56:5), yet as indicated previously, no differences in the total fatty acid composition was found in the seeds. Although, differences in the content of some lipid species were detected, these were not based on fatty acids changes but rather on their distribution into glycerolipid species. These findings are similar to those described previously (Martins-Noguerol et al., 2020), where the overexpression of plastidial lipoyl synthase forms from sunflower in Arabidopsis seeds produced changes in lipid species without altering the total fatty acid content. Thus, the rearrangement of fatty acids into lipid species in transgenic seeds here could be due to modifications in the acyl-CoA pool during seed development.

These data suggest that *Ha*LIP2p1 is able to alter lipid metabolism in Arabidopsis seeds, affecting the oil composition. However, these changes are unpredictable and this offers further evidence of the complexity underlying the regulation of lipid biosynthesis in plants.

5. Conclusion

We discovered two plastidial octanoyltransferases in H. annus, HaLIP2p1 and HaLIP2p2, being HaLIP2p1 the predominant form in the species. In silico models suggest their activity proceed through the formation of an acyl-thioester intermediate between the octanoyl chain and a conserved Cys residue from the enzyme, likewise in other species. HaLIP2p is able to alter lipid metabolism when it is heterologous expressed in bacteria and Arabidopsis seeds. In the latest, overexpression of HaLIP2p produce changes in the content of glycerolipids, including several most abundant TAGs in Arabidopsis seeds, likely due to an excess of LIP2 activity and depletion of plastidial octanoyl-ACP. These findings further our understanding of LIP2 activity in the context of lipid biosynthesis.

CRediT authorship contribution statement

Raquel Martins-Noguerol: Formal analysis, Investigation, Methodology, Writing – original draft, Writing – review & editing. **Sebastien Acket:** Investigation, Methodology. **Manuel Adrián Troncoso-Ponce:** Supervision, Writing – review & editing. **Rafael Garcés:** Project administration. **Mónica Venegas-Calerón:** Writing – review & editing. **Joaquín J. Salas:** Conceptualization, Supervision, Validation, Writing – review & editing. **Enrique Martínez-Force:** Conceptualization, Supervision, Validation, Writing – review & editing. **Antonio Javier Moreno-Pérez:** Data curation, Conceptualization, Supervision, Validation, Writing – review & editing.

Declaration of competing interest

The authors declare that they have no known competing financial interests or personal relationships that could have appeared to influence the work reported in this paper.

Acknowledgements

This work was supported by Spanish State Research Agency Projects AGL 2017-83449-R and PID 2020-113134RBI00, and the CSIC Project I-LINK1186. The authors also wish to thank the Hauts-de-France Region and the European Regional Development Fund (ERDF) 2014/2020 for their funding of this work.

Appendix A. Supplementary data

Supplementary data to this article can be found online at https://doi.org/10.1016/j.jplph.2022.153730.

References

Almagro Armenteros, J.J., Sønderby, C.K., Sønderby, S.K., Nielsen, H., Winther, O., 2017. DeepLoc: prediction of protein subcellular localization using deep learning, 1 Bioinformatics 33 (21), 3387–3395. https://doi.org/10.1093/bioinformatics/btx431.

Alonso, A.P., Goffman, F.D., Ohlrogge, J.B., Shachar-Hill, Y., 2007. Carbon conversion efficiency and central metabolic fluxes in developing (*Helianthus annuus* L.) embryos. Plant J. 52 (2), 296–308. https://doi.org/10.1111/j.1365-313X.2007.03235.x.

Araya-Flores, J., Miranda, S., Covarrubias, M.P., Stange, C., Handford, M., 2020. *Solanum lycopersicum* (tomato) possesses mitochondrial and plastidial lipoyl synthases capable of increasing lipoylation levels when expressed in bacteria. Plant Physiol. Biochem. 151, 264–270. https://doi.org/10.1016/j.plaphy.2020.03.03.

Badouin, H., Gouzy, J., Grassa, C.J., Murat, F., Staton, E., Cottret, L., Lelandais-Brière, C., Owens, G.L., Carrère, S., Mayjonade, B., Legrand, L., Gill, N., Kane, N.C., Bowers, J. E., Hubner, S., Bellec, A., Bérard, A., Bergès, H., Blanchet, N., Boniface, M.C., Brunel, D., Catrice, O., Chaidir, N., Claudel, C., Donnadieu, C., Faraut, T., Fievet, G., Helmstetter, N., King, M., Knapp, S.J., Lai, Z., Le Paslier, M.C., Lippi, Y., Lorenzon, L., Mandel, J.R., Marage, G., Marchand, G., Marquand, E., Bret-Mestries, E., Morien, E., Nambeesan, S., Nguyen, T., Pegot-Espagnet, P., Pouilly, N., Raftis, F., Sallet, E., Schiex, T., Thomas, J., Vandecasteele, C., Varès, D., Vear, F., Vautrin, S., Crespi, M., Mangin, B., Burke, J.M., Salse, J., Muños, S., Vincourt, P., Rieseberg, L.H., Langlade, N.B., 2017. The sunflower genome provides insights into oil metabolism, flowering, and asterid evolution. Nature 546, 148–152. https://doi.org/10.1038/nature22380.

Bannai, H., Tamada, Y., Maruyama, O., Nakai, K., Miyano, S., 2002. Extensive feature detection of N-terminal protein sorting signals. Bioinformatics 18, 298–305. https://doi.org/10.1093/bioinformatics/18.2.298.

Camacho, C., Coulouris, G., Avagyan, V., Ma, N., Papadopoulos, J., Bealer, K., Madden, T.L., 2009. BLAST+: architecture and applications. BMC Bioinf. 10 (1), 1–9. https://doi.org/10.1186/1471-2105-10-421.

Cronan, J.E., 2016. Assembly of lipoic acid on its cognate enzymes: an extraordinary and essential biosynthetic pathway. Microbiol. Mol. Biol. Rev. 80, 429–450. https://doi.org/10.1128/MMBR.00073-15.

Emanuelsson, O., Brunak, S., von Heijne, G., Nielsen, H., 2007. Locating proteins in the cell using TargetP, SignalP, and related tools. Nat. Protoc. 2, 953–971. https://doi.org/10.1038/nprot.2007.131.

Ewald, R., Hoffmann, C., Florian, A., Neuhaus, E., Fernie, A.R., Bauwe, H., 2014a. Lipoate-protein ligase and octanoyltransferase are essential for protein lipoylation in mitochondria of Arabidopsis. Plant Physiol. 165, 978–990. https://doi.org/10.1104/pp.114.238311.

Ewald, R., Hoffmann, C., Neuhaus, E., Bauwe, H., 2014b. Two redundant octanoyltransferases and one obligatory lipoyl synthase provide protein lipoylation autonomy to plastids of Arabidopsis. Plant Biol. 16, 35–42. https://doi.org/10.1111/plb.12028.

Garcés, R., Mancha, M., 1993. One-step lipid extraction and fatty acid methyl esters preparation from fresh plant tissues. Anal. Biochem. 211 (1), 139–143. https://doi.org/10.1006/abio.1993.1244.

Giordani, T., Cavallini, A., Natali, L., 2014. The repetitive component of the sunflower genome. Curr. Plant Biol. 1, 45–54. https://doi.org/10.1016/j.cpb.2014.05.001.

González-Mellado, D., von Wettstein-Knowles, P., Garcés, R., Martínez-Force, E., 2010. The role of beta-ketoacyl-acyl carrier protein synthase III in the condensation steps of fatty acid biosynthesis in sunflower. Planta 231, 1277–1289. https://doi.org/10.1007/s00425-010-1131-z.

González-Thuillier, I., Venegas-Calerón, M., Sánchez, R., Garcés, R., von Wettstein-Knowles, P., Martínez-Force, E., 2016. Sunflower (*Helianthus annuus*) fatty acid synthase complex: β-hydroxyacyl-[acyl carrier protein] dehydratase genes. Planta 243 (2), 397–410. https://doi.org/10.1007/s00425-015-2410-5.

Grosdidier, A., Zoete, V., Michielin, O., 2011a. Fast docking using the CHARMM force field with EADock DSS. J. Comput. Chem. 32, 2149–2159. https://doi.org/10.1002/jcc.21797.

Grosdidier, A., Zoete, V., Michielin, O., 2011b. SwissDock, a protein-small molecule docking web service based on EADock DSS. Nucleic Acids Res. 39, 270–277. https://doi.org/10.1093/nar/gkr366.

Hall, T., 1999. BioEdit: a user-friendly biological sequence alignment editor and analysis program for Windows 95/98/NT. Nucleic Acids Symp. Ser. 41, 95–98.

Harrison, S.J., Mott, E.K., Parsley, K., Aspinall, S., Gray, J.C., Cottage, A., 2006. A rapid and robust method of identifying transformed *Arabidopsis thaliana* seedlings following floral dip transformation. Plant Methods 2, 19. https://doi.org/10.1186/1746-4811-2-19.

von Heijne, G., Steppuhn, J., Herrmann, R.G., 1989. Domain structure of mitochondrial and chloroplast targeting peptides. Eur. J. Biochem. 180 (3), 535–545. https://doi.org/10.1111/j.1432-1033.1989.tb14679.x.

Kang, S.G., Jeong, H.K., Lee, E., Natarajan, S., 2007. Characterization of a lipoate-protein ligase. A gene of rice (*Oryza sativa* L.). Gene 393, 53–61. https://doi.org/10.1016/j.gene.2007.01.011.

Kind, T., Liu, K.H., Lee, D.Y., DeFelice, B., Meissen, J.K., Fiehn, O., 2013. LipidBlast in silico tandem mass spectrometry database for lipid identification. Nat. Methods 10 (8), 755–758. https://doi.org/10.1038/nmeth.2551.

Koelmel, J.P., Kroeger, N.M., Ulmer, C.Z., Bowden, J.A., Patterson, R.E., Cochran, J.A., Beecher, C., Garrett, T.J., Yost, R.A., 2017. LipidMatch: an automated workflow for rule-based lipid identification using untargeted high-resolution tandem mass spectrometry data. BMC Bioinf. 18 (1), 331. https://doi.org/10.1186/s12859-017-1744-3.

Larkin, M.A., Blackshields, G., Brown, N.P., Chenna, R., McGettigan, P.A., McWilliam, H., Valentin, F., Wallace, I.M., Wilm, A., Lopez, R., Thompson, J.D., Gibson, T.J., Higgins, D.G., 2007. Clustal W and clustal X version 2.0. Bioinformatics 23 (21), 2947–2948. https://doi.org/10.1093/bioinformatics/btm404.

Ma, Q., Zhao, X., Eddine, A.N., Geerlof, A., Li, X., Cronan, J.E., Kaufmann, S.H., Wilmanns, M., 2006. The mycobacterium tuberculosis LipB enzyme functions as a cysteine/lysine dyad acyltransferase. Proc. Natl. Acad. Sci. U.S.A. 103, 8662–8667. https://doi.org/10.1073/pnas.0510436103.

Martins-Noguerol, R., Moreno-Pérez, A.J., Acket, S., Makni, S., Garcés, R., Troncoso-Ponce, M.A., Salas, J.J., Thomasset, B., Martínez-Force, E., 2019. Lipidomic analysis of plastidial octanoyltransferase mutants of *Arabidopsis thaliana*. Metabolites 9 (10), 209. https://doi.org/10.3390/metabo9100209.

Martins-Noguerol, R., Moreno-Pérez, A.J., Sebastien, A., Troncoso-Ponce, M.A., Garcés, R., Thomasset, B., Salas, J.J., Martínez-Force, E., 2020. Impact of sunflower (*Helianthus annuus* L.) plastidial lipoyl synthases genes expression in glycerolipids composition of transgenic Arabidopsis plants. Sci. Rep. 10 (1), 1–16. https://doi.org/10.1038/s41598-020-60686-z.

Martins-Noguerol, R., Acket, S., Troncoso-Ponce, M.A., Garcés, R., Thomasset, B., Venegas-Calerón, M., Salas, J.J., Martínez-Force, E., Moreno-Pérez, A.J., 2021. Characterization of *Helianthus annuus* lipoic acid biosynthesis: the mitochondrial octanoyltransferase and lipoyl synthase enzyme system. Front. Plant Sci. 12, 781917. https://doi.org/10.3389/fpls.2021.781917.

Ohlrogge, J.B., Kuhn, D.N., Stumpf, P.K., 1979. Subcellular localization of acyl carrier protein in leaf protoplasts of *Spinacia oleracea*. Proc. Natl. Acad. Sci. U.S.A. 76 (3), 1194–1198. https://doi.org/10.1073/pnas.76.3.1194.

Pettersen, E.F., Goddard, T.D., Huang, C.C., Couch, G.S., Greenblatt, D.M., Meng, E.C., Ferrin, T.E., 2004. UCSF Chimera-a visualization system for exploratory research and analysis. J. Comput. Chem. 25, 1605–1612. https://doi.org/10.1002/jcc.20084.

Reed, L.J., Hackert, M.L., 1966. Chemistry and function of lipoic Acid. Compr. Biochem. 14, 99–126. https://doi.org/10.1002/9780470122631.ch8.

Sayanova, O., Haslam, R., Venegas-Calerón, M., Napier, J.A., 2006. Identification of Primula "front-end" desaturases with distinct n−6 or n−3 substrate preferences. Planta 224 (6), 1269–1277. https://doi.org/10.1007/s00425-006-0306-0.

Schwede, T., Kopp, J., Guex, N., Peitsch, M.C., 2003. SWISS-MODEL: an automated protein homology-modeling server. Nucleic Acids Res. 31, 3381–3385. https://doi.org/10.1093/nar/gkg520.

Schwender, J., Goffman, F., Ohlrogge, J.B., Shachar-Hill, Y., 2004. Rubisco without the Calvin cycle improves the carbon efficiency of developing green seeds. Nature 432 (7018), 779–782. https://doi.org/10.1038/nature03145.

Serrano-Vega, M.J., Garcés, R., Martínez-Force, E., 2005. Cloning, characterization and structural model of a FatA-type thioesterase from sunflower seeds (*Helianthus annuus* L.). Planta 221, 868–880. https://doi.org/10.1007/s00425-005-1502-z.

Small, I., Peeters, N., Legeai, F., Lurin, C., 2004. Predotar: a tool for rapidly screening proteomes for N-terminal targeting sequences. Proteomics 4, 1581–1590. https://doi.org/10.1002/pmic.200300776.

Takami, T., Shibata, M., Kobayashi, Y., Shikanai, T., 2010. De novo biosynthesis of fatty acids plays critical roles in the response of the photosynthetic machinery to low temperature in Arabidopsis. Plant Cell Physiol. 51 (8), 1265–1275. https://doi.org/10.1093/pcp/pcq085.

Tamura, K., Stecher, G., Peterson, D., Filipski, A., Kumar, S., 2013. MEGA6: molecular evolutionary genetics analysis version 6.0. Mol. Biol. Evol. 30, 2725–2729. https://doi.org/10.1093/molbev/mst197.

Ulmer, C.Z., Patterson, R.E., Koelmel, J.P., Garrett, T.J., Yost, R.A., 2017. A robust lipidomics workflow for mammalian cells, plasma, and tissue using liquid-chromatography high-resolution tandem mass spectrometry. In: Bhattacharya, S.K. (Ed.), Lipidomics: Methods and Protocols, Methods in Molecular Biology. Springer, New York, NY, USA, pp. 91–106.

Vanden Boom, T.J., Reed, K.E., Cronan Jr., J.E., 1991. Lipoic acid metabolism in *Escherichia coli*: isolation of null mutants defective in lipoic acid biosynthesis, molecular cloning and characterization of the E. coli lip locus, and identification of the lipoylated protein of the glycine cleavage system. J. Bacteriol. 173, 6411–6420. https://doi.org/10.1128/jb.173.20.6411-6420.1991.

Venegas-Calerón, M., Muro-Pastor, A.M., Garcés, R., Martínez-Force, E., 2006. Functional characterization of a plastidial omega-3 desaturase from sunflower (*Helianthus annuus*) in cyanobacteria. Plant Physiol. Biochem. 44, 517–525. https://doi.org/10.1016/j.plaphy.2006.09.005.

Wada, M., Yasuno, R., Jordan, S.W., Cronan, J.E., Wada, H., 2001. Lipoic acid metabolism in *Arabidopsis thaliana*: cloning and characterization of a cDNA encoding lipoyltransferase. Plant Cell Physiol. 42, 650–656. https://doi.org/10.1093/pcp/pce081.

Wilson, R.L., Stauffer, L.T., Stauffer, G.V., 1993. Roles of the GcvA and PurR proteins in negative regulation of the *Escherichia coli* glycine cleavage enzyme system. J. Bacteriol. 175 (16), 5129–5134. https://doi.org/10.1128/jb.175.16.5129-5134.1993.

Wu, G.Z., Xue, H.W., 2010. Arabidopsis β-ketoacyl-[acyl carrier protein] synthase I is crucial for fatty acid synthesis and plays a role in chloroplast division and embryo development. Plant Cell 22 (11), 3726–3744. https://doi.org/10.1105/tpc.110.075564.

Yasuno, R., Wada, H., 1998. Biosynthesis of lipoic acid in Arabidopsis: cloning and characterization of the cDNA for lipoic acid synthase. Plant Physiol. 118, 935–943. https://doi.org/10.1104/pp.118.3.935.

Yasuno, R., Wada, H., 2002. The biosynthetic pathway for lipoic acid is present in plastids and mitochondria in *Arabidopsis thaliana*. FEBS Lett. 517 (1–3), 110–114.

Zhang, X.P., Glaser, E., 2002. Interaction of plant mitochondrial and chloroplast signal peptides with the Hsp70 molecular chaperone. Trends Plant Sci. 7 (1), 14–21. https://doi.org/10.1016/S1360-1385(01)02180-X.

Zhao, X., Miller, J.R., Jiang, Y., Marletta, M.A., Cronan, J.E., 2003. Assembly of the covalent linkage between lipoic acid and its cognate enzymes. Chem. Biol. 10, 1293–1302. https://doi.org/10.1016/j.chembiol.2003.11.016.

Zhao, X., Miller, J.R., Cronan, J.E., 2005. The reaction of LipB, the octanoyl-[Acyl carrier protein]:Protein N-octanoyltransferase of lipoic acid synthesis, proceeds through an acyl-enzyme intermediate. Biochemistry 44 (50), 16737–16746. https://doi.org/10.1021/bi051865y.